

Extracting the Sivers function from polarized SIDIS data and making predictions

M. Anselmino¹, M. Boglione¹, U. D'Alesio², A. Kotzinian³, F. Murgia², A. Prokudin¹

¹*Dipartimento di Fisica Teorica, Università di Torino and
INFN, Sezione di Torino, Via P. Giuria 1, I-10125 Torino, Italy*

²*INFN, Sezione di Cagliari and Dipartimento di Fisica, Università di Cagliari,
C.P. 170, I-09042 Monserrato (CA), Italy*

³*Dipartimento di Fisica Generale, Università di Torino and
INFN, Sezione di Torino, Via P. Giuria 1, I-10125 Torino, Italy*

Abstract

The most recent data on the weighted transverse single spin asymmetry $A_{UT}^{\sin(\phi_h - \phi_S)}$ from HERMES and COMPASS collaborations are analysed within LO parton model with unintegrated parton distribution and fragmentation functions; all transverse motions are taken into account, with exact kinematics, in the elementary interactions. The overall quality of the data is such that, for the first time, a rather well constrained extraction of the Sivers function for u and d quarks is possible and is performed. Comparisons with models are made. Based on the extracted Sivers functions, predictions for $A_{UT}^{\sin(\phi_h - \phi_S)}$ asymmetries at JLab are given; suggestions for further measurements at COMPASS, with a transversely polarized hydrogen target and selecting favourable kinematical ranges, are discussed. Predictions are also presented for Single Spin Asymmetries (SSA) in Drell-Yan processes at RHIC and GSI.

1. Introduction

In a recent paper [1] we have discussed the role of intrinsic motions in inclusive and Semi-Inclusive Deep Inelastic Scattering (SIDIS) processes, both in unpolarized and polarized $\ell p \rightarrow \ell h X$ reactions. The LO QCD parton model computations have been compared with the experimental dependence of the unpolarized cross section on the azimuthal angle, around the virtual photon direction, between the leptonic and the hadronic planes (Cahn effect [2]); at small transverse momentum P_T of the produced hadron h , such an effect is dominantly related to intrinsic motions and it allows an estimate of the average values of the transverse momenta of quarks inside a proton, \mathbf{k}_\perp , and of final hadrons inside the fragmenting quark jet, \mathbf{p}_\perp , with the best fit results:

$$\langle k_\perp^2 \rangle = 0.25 \text{ (GeV}/c)^2 \quad \langle p_\perp^2 \rangle = 0.20 \text{ (GeV}/c)^2. \quad (1)$$

More detail, both about the kinematical configurations and conventions [3] and the fitting procedure can be found in Ref. [1]. We only notice here that the above values have been derived from sets of data collected at different energies and in different ranges of the kinematical variables x_B , Q^2 and z_h , looking at the combined production of all charged hadrons in SIDIS processes; constant and flavour independent values of $\langle k_\perp^2 \rangle$ and $\langle p_\perp^2 \rangle$ have been assumed, avoiding at this stage complications related to possible x , z and Q^2 dependences. Rather than a definite derivation, the above results are better considered as a consistent simple estimate and a convenient parameterization of the true intrinsic motion of quarks in nucleons and of hadrons in jets, supported by the available experimental information.

Equipped with such estimates, in Ref. [1] we have studied the transverse single spin asymmetries $A_{UT}^{\sin(\phi_\pi - \phi_S)}$ observed by HERMES collaboration [4]; that allowed a first rough extraction of the Sivers function [5]

$$\Delta^N f_{q/p^\dagger}(x, k_\perp) = -\frac{2 k_\perp}{m_p} f_{1T}^{\perp q}(x, k_\perp), \quad (2)$$

defined by

$$f_{q/p^\dagger}(x, \mathbf{k}_\perp) = f_{q/p}(x, k_\perp) + \frac{1}{2} \Delta^N f_{q/p^\dagger}(x, k_\perp) \mathbf{S} \cdot (\hat{\mathbf{P}} \times \hat{\mathbf{k}}_\perp) \quad (3)$$

$$= f_{q/p}(x, k_\perp) - f_{1T}^{\perp q}(x, k_\perp) \frac{\mathbf{S} \cdot (\hat{\mathbf{P}} \times \mathbf{k}_\perp)}{m_p}, \quad (4)$$

where $f_{q/p}(x, k_\perp)$ is the unpolarized x and k_\perp dependent parton distribution ($k_\perp = |\mathbf{k}_\perp|$); m_p , \mathbf{P} and \mathbf{S} are respectively the proton mass, momentum and transverse polarization vectors ($\hat{\mathbf{P}}$ and $\hat{\mathbf{k}}_\perp$ denote unit vectors).

The Sivers function extracted from HERMES data in [1] was shown to be consistent with preliminary COMPASS data on $A_{UT}^{\sin(\phi_h - \phi_S)}$ obtained on a deuteron target, in a different kinematical region [6].

While the preliminary HERMES data [4] offered a definite indication of a non zero Sivers effect, their amount and quality were not yet such that an accurate extraction of the Sivers functions was possible; that reflects in the values of the parameters of the Sivers functions given in Table I of Ref. [1], which have large uncertainties.

New HERMES data are now available [7]; they are consistent with the previous ones, with much smaller errors. Similarly, COMPASS collaboration published [8] their preliminary results. We consider here these whole new sets of HERMES and COMPASS data and perform a novel fit of the Sivers functions. It turns out that the new data constrain much better the parameters, thus offering the first direct significant estimate of the Sivers functions – for u and d quarks – active in SIDIS processes. The sea quark contributions are found to be negligible, at least in the kinematical region of the available data.

The modeled and extracted Sivers functions $\Delta^N f_{u/p^\uparrow}(x, k_\perp)$ and $\Delta^N f_{d/p^\uparrow}(x, k_\perp)$ are used to compute, and thus predict, the values of $A_{UT}^{\sin(\phi_h - \phi_S)}$ expected at COMPASS, for scattering off a polarized hydrogen (rather than deuteron) target, which avoids cancellations between the opposite u and d contributions. Suggestions for the selection of favourable kinematic regions, where the asymmetry is sizeable, are discussed. Similar predictions, with strongly encouraging results, are given for polarized SIDIS processes at JLab.

Finally, we exploit the QCD prediction [9]

$$f_{1T}^{\perp q}(x, k_\perp)|_{\text{DIS}} = -f_{1T}^{\perp q}(x, k_\perp)|_{\text{D-Y}} \quad (5)$$

and compute a single spin asymmetry, which can only originate from the Sivers mechanism [10], for Drell-Yan processes at RHIC and GSI.

2. Extracting the Sivers functions

Following Ref. [1], the inclusive ($\ell p \rightarrow \ell X$) unpolarized DIS cross section in non collinear LO parton model is given by

$$\frac{d^2 \sigma^{\ell p \rightarrow \ell X}}{dx_B dQ^2} = \sum_q \int d^2 \mathbf{k}_\perp f_q(x, k_\perp) \frac{d\hat{\sigma}^{\ell q \rightarrow \ell q}}{dQ^2} J(x_B, Q^2, k_\perp), \quad (6)$$

and the semi-inclusive one ($\ell p \rightarrow \ell h X$) by

$$\frac{d^5 \sigma^{\ell p \rightarrow \ell h X}}{dx_B dQ^2 dz_h d^2 \mathbf{P}_T} = \sum_q \int d^2 \mathbf{k}_\perp f_q(x, k_\perp) \frac{d\hat{\sigma}^{\ell q \rightarrow \ell q}}{dQ^2} J \frac{z}{z_h} D_q^h(z, p_\perp), \quad (7)$$

where

$$J = \frac{\hat{s}^2}{x_B^2 s^2} \frac{x_B}{x} \left(1 + \frac{x_B^2 k_\perp^2}{x^2 Q^2} \right)^{-1} \quad (8)$$

and

$$\frac{d\hat{\sigma}^{\ell q \rightarrow \ell q}}{dQ^2} = e_q^2 \frac{2\pi\alpha^2}{\hat{s}^2} \frac{\hat{s}^2 + \hat{u}^2}{Q^4}. \quad (9)$$

Q^2 , x_B and $y = Q^2/(x_B s)$ are the usual leptonic DIS variables and z_h, \mathbf{P}_T the usual hadronic SIDIS ones, in the γ^*p c.m. frame; x and z are light-cone momentum fractions, with (see Ref. [1] for exact relationships and further detail):

$$x = x_B + \mathcal{O}\left(\frac{k_\perp^2}{Q^2}\right) \quad z = z_h + \mathcal{O}\left(\frac{k_\perp^2}{Q^2}\right) \quad \mathbf{p}_\perp = \mathbf{P}_T - z_h \mathbf{k}_\perp + \mathcal{O}\left(\frac{k_\perp^2}{Q^2}\right). \quad (10)$$

The elementary Mandelstam variables are given by

$$\hat{s}^2 = \frac{Q^4}{y^2} \left[1 - 4 \frac{k_\perp}{Q} \sqrt{1-y} \cos \varphi \right] + \mathcal{O}\left(\frac{k_\perp^2}{Q^2}\right) \quad (11)$$

$$\hat{u}^2 = \frac{Q^4}{y^2} (1-y)^2 \left[1 - 4 \frac{k_\perp}{Q} \frac{\cos \varphi}{\sqrt{1-y}} \right] + \mathcal{O}\left(\frac{k_\perp^2}{Q^2}\right), \quad (12)$$

where φ is the azimuthal angle of the quark transverse momentum, $\mathbf{k}_\perp = k_\perp(\cos \varphi, \sin \varphi, 0)$. Regarding angle definitions and notations we adopt throughout the paper the so-called ‘‘Trento conventions’’ [3] (see also Fig. 3 of Ref. [1]).

The $\sin(\phi_h - \phi_S)$ weighted transverse single spin asymmetry, measured by HERMES and COMPASS, which singles out the contribution of the Sivers function (2), is given by:

$$A_{UT}^{\sin(\phi_h - \phi_S)} = \frac{\sum_q \int d\phi_S d\phi_h d^2\mathbf{k}_\perp \Delta^N f_{q/p^\dagger}(x, k_\perp) \sin(\varphi - \phi_S) \frac{d\hat{\sigma}^{\ell q \rightarrow \ell q}}{dQ^2} J \frac{z}{z_h} D_q^h(z, p_\perp) \sin(\phi_h - \phi_S)}{\sum_q \int d\phi_S d\phi_h d^2\mathbf{k}_\perp f_{q/p}(x, k_\perp) \frac{d\hat{\sigma}^{\ell q \rightarrow \ell q}}{dQ^2} J \frac{z}{z_h} D_q^h(z, p_\perp)}. \quad (13)$$

We shall use Eq. (13), in which we insert a parameterization for the Sivers functions, to fit the experimental data.

We adopt the usual (and convenient) gaussian factorization for the distribution and fragmentation functions:

$$f_{q/p}(x, k_\perp) = f_q(x) \frac{1}{\pi \langle k_\perp^2 \rangle} e^{-k_\perp^2 / \langle k_\perp^2 \rangle} \quad (14)$$

and

$$D_q^h(z, p_\perp) = D_q^h(z) \frac{1}{\pi \langle p_\perp^2 \rangle} e^{-p_\perp^2 / \langle p_\perp^2 \rangle}, \quad (15)$$

with the values of $\langle k_\perp^2 \rangle$ and $\langle p_\perp^2 \rangle$ of Eq. (1). Isospin and charge-conjugation relations imply

$$\begin{aligned} D_u^{\pi^+}(z) &= D_d^{\pi^-}(z) = D_{\bar{u}}^{\pi^-}(z) = D_{\bar{d}}^{\pi^+}(z) \equiv D_{\text{fav}}(z) \\ D_u^{\pi^-}(z) &= D_d^{\pi^+}(z) = D_{\bar{u}}^{\pi^+}(z) = D_{\bar{d}}^{\pi^-}(z) \equiv D_{\text{unfav}}(z). \end{aligned} \quad (16)$$

The integrated parton distribution and fragmentation functions $f_q(x)$ and $D_q^h(z)$ are taken from the literature, at the appropriate Q^2 values of the experimental data [11, 12].

We parameterize, for each light quark flavour $q = u, d, \bar{u}, \bar{d}$, the Siverson function in the following factorized form:

$$\Delta^N f_{q/p^\dagger}(x, k_\perp) = 2 \mathcal{N}_q(x) h(k_\perp) f_{q/p}(x, k_\perp) , \quad (17)$$

where

$$\mathcal{N}_q(x) = N_q x^{a_q} (1-x)^{b_q} \frac{(a_q + b_q)^{(a_q + b_q)}}{a_q^{a_q} b_q^{b_q}} , \quad (18)$$

$$h(k_\perp) = \frac{2k_\perp M_0}{k_\perp^2 + M_0^2} . \quad (19)$$

N_q , a_q , b_q and M_0 (GeV/c) are free parameters. $f_{q/p}(x, k_\perp)$ is the unpolarized distribution function defined in Eq. (14). Since $h(k_\perp) \leq 1$ and since we allow the constant parameter N_q to vary only inside the range $[-1, 1]$ so that $|\mathcal{N}_q(x)| \leq 1$ for any x , the positivity bound for the Siverson function is automatically fulfilled:

$$\frac{|\Delta^N f_{q/p^\dagger}(x, k_\perp)|}{2f_{q/p}(x, k_\perp)} \leq 1 . \quad (20)$$

We have first attempted a fit of the HERMES and COMPASS data, taking into account 4 Siverson functions (for u, d, \bar{u} and \bar{d} quarks), for a total of 13 parameters, like in Ref. [1]. However, it turns out that the available data are almost insensitive to the sea quark (and, in general, small x) contributions, which leads to largely undetermined parameters of the corresponding Siverson functions. Indeed, we have explicitly checked that various choices of $\Delta^N f_{\bar{u}/p^\dagger}$ and $\Delta^N f_{\bar{d}/p^\dagger}$ do not significantly affect the computation of $A_{UT}^{\sin(\phi_h - \phi_S)}$, Eq. (13), in the kinematical regions of the performed experiments. We have then neglected the contributions of these functions and considered only the contributions of $\Delta^N f_{u/p^\dagger}$ and $\Delta^N f_{d/p^\dagger}$, for a total of 7 free parameters:

$$N_u \quad a_u \quad b_u \quad N_d \quad a_d \quad b_d \quad M_0. \quad (21)$$

The results of our fits are shown in Figs. 1 and 2. The weighted SSA $A_{UT}^{\sin(\phi_h - \phi_S)}$ is plotted as a function of one variable at a time, either z_h or x_B or P_T ; an integration over the other variables has been performed consistently with the cuts of the corresponding experiment (see Ref. [1] for further detail). The resulting best fit values of the parameters are reported in Table I. The shaded area in Figs. 1 and 2 corresponds to one-sigma deviation at 90% CL and was calculated using the errors (Table I) and the correlation matrix generated by MINUIT, minimizing and maximizing the function under consideration, in a 7-dimensional parameter space hyper-volume corresponding to one-sigma deviation.

$N_u =$	0.32 ± 0.11	$N_d =$	-1.00 ± 0.12
$a_u =$	0.29 ± 0.35	$a_d =$	1.16 ± 0.47
$b_u =$	0.53 ± 3.58	$b_d =$	3.77 ± 2.59
$M_0^2 =$	$0.32 \pm 0.25 \text{ (GeV}/c)^2$	$\chi^2/d.o.f. =$	1.06

Table I: Best fit values of the parameters of the Siverson functions. Notice that the errors generated by MINUIT are strongly correlated, and should not be taken at face value; the significant fluctuations in our results are shown by the shaded areas in Figs. 1 and 2.

In Fig. 1 we also show predictions, obtained using the extracted Siverson functions, for π^0 and K production; data on these asymmetries might be available soon from HERMES collaboration.

3. Comparison with models and predictions for SIDIS processes

The extracted Siverson functions for u and d quarks are shown in Fig. 3, where we plot, for comparison with other results, the first \mathbf{k}_\perp moment

$$\Delta^N f_q^{(1)}(x) \equiv \int d^2 \mathbf{k}_\perp \frac{k_\perp}{4m_p} \Delta^N f_{q/p^\uparrow}(x, k_\perp) = -f_{1T}^{\perp(1)q}(x). \quad (22)$$

The solid line corresponds to the central values in Table I and the shaded area corresponds to varying the parameters within the shaded areas in Figs. 1 and 2. The other curves show results from models or fits to different data [13, 14, 15], as discussed below.

- The x -dependences of both $\Delta^N f_{u/p^\uparrow}$ and $\Delta^N f_{d/p^\uparrow}$ – as modeled in Eqs. (17-19) and shown in Fig. 3 – appear to be rather well determined, keeping in mind that the data are essentially confined in the region $0.01 \lesssim x_B \lesssim 0.2$. We notice that a 13-parameter fit – including \bar{u} and \bar{d} contributions – would lead to similar results; however, the values of $\Delta^N f_{\bar{u}/p^\uparrow}$ and $\Delta^N f_{\bar{d}/p^\uparrow}$, within their shaded areas, would be consistent with zero in the kinematical region of HERMES and COMPASS experiments. That is why we have not considered these contributions here.
- The large- x behaviour of the Siverson functions cannot be fixed by the existing data. According to the counting rules of Ref. [16], and keeping in mind that $\Delta^N f_{q/p^\uparrow}$ originates from the interference between *distribution amplitudes* with different proton helicities [17, 18], one expects the large- x behaviours

$$\Delta^N f_{u/p^\uparrow} \sim \Delta^N f_{d/p^\uparrow} \sim (1-x)^4. \quad (23)$$

JLab data will cover the appropriate region to help checking this prediction.

- The dot-dashed line in Fig. 3 shows fit I of Ref. [13], where the q_T/m_p weighted SIDIS asymmetries were fitted and the large N_c relation [19, 20] was adopted:

$$f_{1T}^{\perp u}(x, k_{\perp}) = -f_{1T}^{\perp d}(x, k_{\perp}) . \quad (24)$$

Notice that their results are in qualitative agreement with ours and that Eq. (24) naturally turns out to be approximately true in our fit.

- The dashed line in Fig. 3 plots the first \mathbf{k}_{\perp} moment of the Sivers functions obtained in Ref. [14], by fitting A_N data in $p^{\uparrow} p \rightarrow \pi X$ processes; these data are mainly sensitive to large x value, where – again – approximately opposite values of $\Delta^N f_{u/p^{\uparrow}}$ and $\Delta^N f_{d/p^{\uparrow}}$ seem to be favoured. However, as discussed in Ref. [1], the universality of the Sivers functions active in SIDIS and $p^{\uparrow} p \rightarrow \pi X$ processes is still an open issue.
- Most theoretical models give a Sivers function for u quarks much larger, in magnitude, than for d quarks; this can be seen, for example, from the dotted curve in Fig. 3, taken from the computation, in the MIT bag model, of Ref. [15]. The same is true for the Sivers functions obtained, within a spectator model with diquarks, in Refs. [21], [22] and [23].

3.1 $A_{UT}^{\sin(\phi_h - \phi_S)}$ at COMPASS with polarized hydrogen target

By inspection of Eq. (13) it is easy to understand our numerical results for the u and d Sivers functions. In fact one can see that for scattering off a hydrogen target (HERMES), one has

$$\left(A_{UT}^{\sin(\phi_h - \phi_S)}\right)_{\text{hydrogen}} \sim 4 \Delta^N f_{u/p^{\uparrow}} D_u^h + \Delta^N f_{d/p^{\uparrow}} D_d^h , \quad (25)$$

while, for a scattering off a deuterium target (COMPASS),

$$\left(A_{UT}^{\sin(\phi_h - \phi_S)}\right)_{\text{deuterium}} \sim \left(\Delta^N f_{u/p^{\uparrow}} + \Delta^N f_{d/p^{\uparrow}}\right) \left(4 D_u^h + D_d^h\right) . \quad (26)$$

Opposite u and d Sivers contributions suppress COMPASS asymmetries for any hadron h . These opposite contributions do not affect the π^+ asymmetry measured off a a hydrogen target, Eq. (25): in this case the charge factor 4 and the favourite fragmentation function ($D_u^{\pi^+} > D_d^{\pi^+}$) combine to make the first term of Eq. (25) larger than the second one. The cancellation between the two terms is stronger for the π^- asymmetry, because in this case the charge factor 4 in the first term of Eq. (25) couples to the unfavoured fragmentation function ($D_u^{\pi^-} < D_d^{\pi^-}$). Similar arguments hold for the production of kaons and, in general, for the production of charged hadrons, which is dominated by pions.

However, the COMPASS collaboration will soon be taking data with a transversely polarized hydrogen target. We can easily compute the expected results:

adopting the same experimental cuts which were used for the deuterium target [1] we obtain the predictions shown in the upper panel of Fig. 4. The asymmetry is found to be around 5%. These expected values can be further increased by properly selecting the experimental data, thus excluding kinematical regions whose contribution to the asymmetry is negligible. For example, selecting events with

$$0.4 \leq z_h \leq 1 \quad 0.2 \leq P_T \leq 1 \text{ GeV}/c \quad 0.02 \leq x_B \leq 1, \quad (27)$$

yields the predictions shown in the lower panel of Fig. 4. The asymmetry for positively charged hadrons becomes larger, and, provided that enough statistics can be gathered, one expects a clear observation of a sizeable azimuthal asymmetry also for the COMPASS experiment.

3.2 $A_{UT}^{\sin(\phi_h - \phi_S)}$ at JLab with polarized hydrogen target

Also JLab experiments are supposed to measure the SIDIS azimuthal asymmetry for the production of pions on a transversely polarised hydrogen target, at incident beam energies of 6 and 12 GeV. The kinematical region of this experiment is very interesting, as it will supply information on the behaviour of the Sivers functions in the large- x_B domain, up to $x_B \simeq 0.6$. The experimental acceptance for JLab events at 6 GeV is constrained by [24]:

$$\begin{aligned} 0.4 \leq z_h \leq 0.7 & \quad 0.02 \leq P_T \leq 1 \text{ GeV}/c & \quad 0.1 \leq x_B \leq 0.6 & \quad (28) \\ 0.4 \leq y \leq 0.85 & \quad Q^2 \geq 1 \text{ (GeV}/c)^2 & \quad W^2 \geq 4 \text{ GeV}^2 & \quad 1 \leq E_h \leq 4 \text{ GeV}. \end{aligned}$$

while, with an incident beam energy of 12 GeV, this becomes:

$$\begin{aligned} 0.4 \leq z_h \leq 0.7 & \quad 0.02 \leq P_T \leq 1.4 \text{ GeV}/c & \quad 0.05 \leq x_B \leq 0.7 & \quad (29) \\ 0.2 \leq y \leq 0.85 & \quad Q^2 \geq 1 \text{ (GeV}/c)^2 & \quad W^2 \geq 4 \text{ GeV}^2 & \quad 1 \leq E_h \leq 7 \text{ GeV}. \end{aligned}$$

Imposing these experimental cuts we obtain the predictions shown in Fig. 5. A large and healthy azimuthal asymmetry for π^+ production should be observed. Similar results have been obtained also in an approach based on a Monte Carlo event generator [25]. However, one relevant comment is in order:

- As the region of high x_B is not covered by HERMES and COMPASS experiments, the predictions for the large- x_B dependence of the asymmetry are very sensitive to the few large- x_B data points of these two experiments. As a consequence, the results for JLab experiments may still change drastically in the region $0.4 \lesssim x_B \lesssim 0.6$, and the asymmetry might be much smaller than presented in Fig. 5. This reflects in the wide shaded area at large x_B values. Conversely, the results on P_T and z_h dependences are more stable as they depend on the x_B -integrated Sivers function. Notice also the little dependence on the beam energy, consistent with the approximate factorized form of the numerator and denominator of Eq. (13), which leads to cancellations in their ratio.

4. Transverse single spin asymmetries in Drell-Yan processes

Let us now consider the transverse single spin asymmetry,

$$A_N = \frac{d\sigma^\uparrow - d\sigma^\downarrow}{d\sigma^\uparrow + d\sigma^\downarrow}, \quad (30)$$

for Drell-Yan processes, $p^\uparrow p \rightarrow \ell^+ \ell^- X$, $p^\uparrow \bar{p} \rightarrow \ell^+ \ell^- X$ and $\bar{p}^\uparrow p \rightarrow \ell^+ \ell^- X$, where $d\sigma$ stands for

$$\frac{d^4\sigma}{dy dM^2 d^2\mathbf{q}_T} \quad (31)$$

and y , M^2 and \mathbf{q}_T are respectively the rapidity, the squared invariant mass and the transverse momentum of the lepton pair in the initial nucleon c.m. system. The cross section can eventually be integrated over some of these variables, according to the kinematical configurations of the experiments.

In such a case the single spin asymmetry (30) can only originate from the Siverts function and is given (selecting the region with $q_T^2 \ll M^2$, $q_T \simeq k_\perp$) by [10]

$$A_N = \frac{\sum_q e_q^2 \int d^2\mathbf{k}_{\perp q} d^2\mathbf{k}_{\perp \bar{q}} \delta^2(\mathbf{k}_{\perp q} + \mathbf{k}_{\perp \bar{q}} - \mathbf{q}_T) \Delta^N f_{q/p^\uparrow}(x_q, \mathbf{k}_{\perp q}) f_{\bar{q}/p}(x_{\bar{q}}, \mathbf{k}_{\perp \bar{q}})}{2 \sum_q e_q^2 \int d^2\mathbf{k}_{\perp q} d^2\mathbf{k}_{\perp \bar{q}} \delta^2(\mathbf{k}_{\perp q} + \mathbf{k}_{\perp \bar{q}} - \mathbf{q}_T) f_{q/p}(x_q, \mathbf{k}_{\perp q}) f_{\bar{q}/p}(x_{\bar{q}}, \mathbf{k}_{\perp \bar{q}})}, \quad (32)$$

where $q = u, \bar{u}, d, \bar{d}, s, \bar{s}$ and

$$x_q = \frac{M}{\sqrt{s}} e^y \quad x_{\bar{q}} = \frac{M}{\sqrt{s}} e^{-y}. \quad (33)$$

Eq. (32) explicitly refers to $p^\uparrow p$ processes, with obvious modifications for $p^\uparrow \bar{p}$ and $\bar{p}^\uparrow p$ ones.

Inserting into Eq. (32) the Siverts functions extracted from our fit to SIDIS data and *reversed in sign* according to Eq. (5), we obtain the predictions shown in Figs. 6 and 7. Fig. 6 shows the value of A_N as a function of M and $x_F = x_q - x_{\bar{q}}$, for RHIC configurations: the lepton pair transverse momentum \mathbf{q}_T has been integrated in the range $0 \leq q_T \leq 1$ GeV/c, while the rapidity variable y and the lepton pair invariant mass M have been integrated according to the experimental situations, as indicated in the legenda. The integration over the azimuthal angle of \mathbf{q}_T has been performed, to avoid cancellations, as in Ref. [10], that is integrating over ϕ_{q_T} in the range $[0, \pi/2]$ only, or, alternatively, taking into account the change of sign in the different production quadrants. In either case, the ϕ_{q_T} integration gives an overall factor $2/\pi$. As the shaded areas in previous figures, the closed areas correspond to the uncertainty in our determination of the Siverts functions.

Fig. 7 shows the same plots for the PAX experiment [26] planned at the proposed asymmetric $p\bar{p}$ collider at GSI: \mathbf{q}_T has been integrated over the same range as for RHIC predictions, while y and M as indicated in the legenda. Results for $p^\uparrow \bar{p}$ and $\bar{p}^\uparrow p$ processes are identical, due to charge conjugation invariance. Notice that in our configuration the polarized proton or antiproton always moves along the $(+\hat{z})$ -direction.

The correct interpretation of these results requires some further considerations.

- In our computations we have used the value of $\langle k_\perp^2 \rangle = 0.25 \text{ (GeV}/c)^2$, obtained from an analysis of SIDIS data [1]; such a value is certainly appropriate for consistently computing spin asymmetries in SIDIS processes, in the γ^*p c.m. frame, as we have done in Section 3.1 and 3.2. This value naturally corresponds to the intrinsic motion of partons confined in a nucleon, simply according to uncertainty principle, and describes well the \mathbf{P}_T dependences of measured cross sections, up to $P_T \simeq 1 \text{ GeV}/c$. In addition, as we have seen, it allows an understanding of the azimuthal asymmetries, which would otherwise vanish.
- However, when considering other processes, as the inclusive production of hadrons or leptons in pp or $p\bar{p}$ interactions, we know that higher order QCD corrections, like the threshold resummation of large logarithms due to soft gluon emission [27], lead to large K -factor enhancements of the cross sections. Our \mathbf{k}_\perp unintegrated approach to the description of hard scattering processes within a generalization of the QCD factorization theorem [14, 28], can be considered as an effective model which not only takes into account the original partonic intrinsic motion (related to parton confinement), but also, to some extent, the intrinsic \mathbf{k}_\perp built via soft gluon emission. Indeed, the values of $\langle k_\perp^2 \rangle$ used in Ref. [14] in order to describe the data on the unpolarized $pp \rightarrow \pi X$ processes are higher than the values used here, and those requested for the Drell-Yan cross-section might be even higher. The average $\langle k_\perp^2 \rangle$ estimate of $0.25 \text{ (GeV}/c)^2$ might be at most adequate to explain the Drell-Yan cross section up to $q_T \lesssim 1 \text{ GeV}/c$, but would badly fail above that value.
- For the reasons explained above, consistently with our approach expected to hold in the $k_\perp \simeq P_T \simeq q_T$ region, in our predictions for A_N , Figs. 6 and 7, we have integrated over \mathbf{q}_T up to $q_T = 1 \text{ GeV}/c$. In addition, we notice that the value of A_N , as given by Eq. (32), is little sensitive to the chosen value of $\langle k_\perp^2 \rangle$: while both the numerator and the denominator of Eq. (32) greatly vary with $\langle k_\perp^2 \rangle$, their ratio does much less so. We then consider our predictions for A_N , assuming the validity of the relation (5), safe and significant.

5. Comments and conclusions

We have considered the most recent data from polarized SIDIS processes which single out the Sivers effect, namely the $A_{UT}^{\sin(\phi_h - \phi_S)}$ transverse single spin azimuthal asymmetry, measured by HERMES [7] and COMPASS [8] collaborations for charged hadron production. Assuming a Gaussian factorization of the k_\perp and p_\perp dependence of all distribution and fragmentation functions, together with a most simple parameterization of the x -dependence of the unknown Sivers functions, we have exploited the data to extract information on $\Delta^N f_{u/p^\uparrow}(x, k_\perp)$ and $\Delta^N f_{d/p^\uparrow}(x, k_\perp)$.

For the first time, the amount and quality of the experimental results allow a significant, although still limited in x -range, estimate of the Sivers functions for u

and d quarks; these turn out to be definitely different from zero, well inside the positivity bound of Eq. (20) and almost opposite to each other. This last feature, predicted theoretically in some models [19, 20], explains naturally and is related to the small asymmetry observed by COMPASS in scatterings of muons off a deuteron target.

According to the general strategy of combining new experimental information with the computation and prediction of new expected results, the extracted functions have been used to compute $A_{UT}^{\sin(\phi_h - \phi_S)}$ in other experiments. It turns out that, contrary to the results obtained off a polarized deuteron target, a sizeable h^+ asymmetry should be measured by COMPASS collaboration once they switch, as planned, to a transversely polarized hydrogen target; a careful choice of the kinematical region of the selected events would help in further increasing the numerical value of the asymmetry for positively charged hadron production.

Large values of $A_{UT}^{\sin(\phi_h - \phi_S)}$ are expected at JLab, both in the 6 and 12 GeV operational modes, for π^+ inclusive production; in particular the z_h and P_T dependence of the asymmetry seems to be stable and reliable, while the x_B dependence shows large uncertainties due to the lack of HERMES and COMPASS information in this region. JLab experiments have the unique features of exploring the large x_B behaviour of the quark distribution functions, where predictions from QCD counting rules, Eq. (23), could be tested.

The Sivers effect was believed for some time to be forbidden by QCD time reversal properties [29]; however, this proved to be incorrect [9] after an explicit model showed the existence of a non zero Sivers function [18]. The original proof of the vanishing of the Sivers effect turned into the relation of Eq. (5), which predicts opposite values for the Sivers functions measured in SIDIS and Drell-Yan processes. We have then used this basic QCD relation and computed the single spin asymmetries in Drell-Yan processes given in Eq. (32); these can only be generated by the Sivers functions, since no fragmentation functions are needed to describe this process. We have used the same functions as extracted from SIDIS data, with opposite signs. The predicted A_N could be measured at RHIC in pp collisions and, in the long range, at the proposed PAX experiment at GSI [26], in $p\bar{p}$ interactions. It would provide a clear and stringent test of basic QCD properties.

A phenomenological study of the Sivers asymmetry – the correlation between the intrinsic \mathbf{k}_\perp of partons and the proton spin – is now possible, thanks to the existing experimental information and more which will soon be available. Basic properties of the QCD proton structure can and will be clarified. A good control of the Sivers mechanism will help in learning and understanding about other fundamental partonic spin properties, like the transversity distribution [30] and the Collins mechanism [29].

Acknowledgements

We would like to thank Elke Aschenauer, Harut Avakian and Delia Hasch for

fruitful discussions. We acknowledge the support of the European Community–Research Infrastructure Activity under the FP6 “Structuring the European Research Area” programme (HadronPhysics, contract number RII3-CT-2004-506078). U.D. and F.M. acknowledge partial support by MIUR (Ministero dell’Istruzione, dell’Università e della Ricerca) under Cofinanziamento PRIN 2003.

References

- [1] M. Anselmino, M. Boglione, U. D’Alesio, A. Kotzinian, F. Murgia and A. Prokudin, *Phys. Rev.* **D71** (2005) 074006
- [2] R.N. Cahn, *Phys. Lett.* **B78** (1978) 269; *Phys. Rev.* **D40** (1989) 3107
- [3] A. Bacchetta, U. D’Alesio, M. Diehl and C.A. Miller, *Phys. Rev.* **D70** (2004) 117504
- [4] HERMES Collaboration, A. Airapetian *et al.*, *Phys. Rev. Lett.* **94** (2005) 012002; U. Elschenbroich, G. Schnell and R. Seidl (on behalf of HERMES Collaboration), e-Print Archive: hep-ex/0405017; talk by N. Makins (on behalf of HERMES Collaboration), Transversity Workshop, Athens, Greece, October 6-7, 2003
- [5] D. Sivers, *Phys. Rev.* **D41** (1990) 83; **D43** (1991) 261
- [6] COMPASS Collaboration, P. Pagano, talk delivered at the SPIN2004 Symposium, Trieste, Italy, October 10-16, 2004, e-Print Archive: hep-ex/0501035
COMPASS Collaboration, R. Webb, talk delivered at BARYONS04, Oct 25-29 2004, Palaiseau, France, e-Print Archive: hep-ex/0501031
- [7] HERMES Collaboration, M. Dieffenthaler, talk delivered at DIS 2005, Madison, Wisconsin (USA), April 27 – May 1, e-Print Archive: hep-ex/0507013
- [8] COMPASS Collaboration, V.Yu. Alexakhin *et al.*, *Phys. Rev. Lett.* **94** (2005) 202002
- [9] J.C. Collins, *Phys. Lett.* **B536** (2002) 43
- [10] M. Anselmino, U. D’Alesio and F. Murgia, *Phys. Rev.* **D67** (2003) 074010
- [11] A.D. Martin, R.G. Roberts, W.J. Stirling and R.S. Thorne, *Phys. Lett.* **B531** (2002) 216
- [12] S. Kretzer, *Phys. Rev.* **D62** (2000) 054001
- [13] A.V. Efremov, K. Goeke, S. Menzel, A. Metz and P. Schweitzer, *Phys. Lett.* **B612** (2005) 233
- [14] U. D’Alesio and F. Murgia, *Phys. Rev.* **D70** (2004) 074009
- [15] F. Yuan, *Phys. Lett.* **B575** (2003) 45
- [16] S.J. Brodsky, M. Burkardt and I. Schmidt, *Nucl. Phys.* **B441** (1995) 197
- [17] M. Anselmino, M. Boglione and F. Murgia, *Phys. Lett.* **B362** (1995) 164
- [18] S.J. Brodsky, D.S. Hwang and I. Schmidt, *Phys. Lett.* **B530** (2002) 99
- [19] M. Anselmino, V. Barone, A. Drago and F. Murgia, e-Print Archive: hep-ph/0209073; A. Drago, *Phys. Rev.* **D71** (2005) 057501
- [20] P.V. Pobilytsa, e-Print Archive: hep-ph/0301236

- [21] A. Bacchetta, A. Schäfer and J-J. Yang, *Phys. Lett.* **B578** (2004) 109
- [22] Z. Lu and B.Q. Ma, *Nucl. Phys.* **A741** (2004) 200
- [23] L.P. Gamberg, G.R. Goldstein and K.A. Oganessyan, *Phys. Rev.* **D67** (2003) 071504
- [24] H. Avakian, private communication
- [25] A. Kotzinian, e-Print Archive: hep-ph/0504081
- [26] PAX Collaboration, e-Print Archive: hep-ex/0505054
- [27] D. de Florian and W. Vogelsang, *Phys. Rev.* **D71** (2005) 114004
- [28] M. Anselmino, M. Boglione, U. D'Alesio E. Leader and F. Murgia, *Phys. Rev.* **D71** (2005) 014002
- [29] J.C. Collins, *Nucl. Phys.* **B396** (1993) 161
- [30] For a comprehensive recent review paper on transversity, see, *e.g.* V. Barone, A. Drago and P. Ratcliffe, *Phys. Rept.* **359** (2002) 1

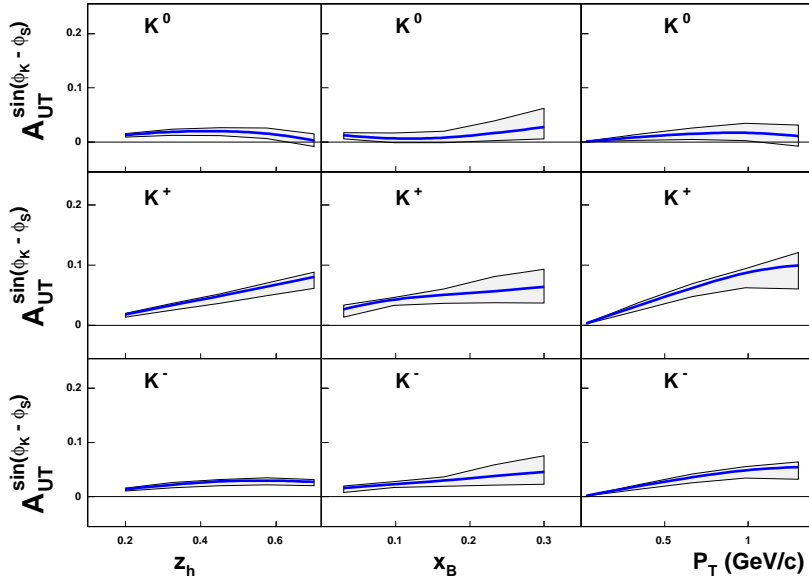
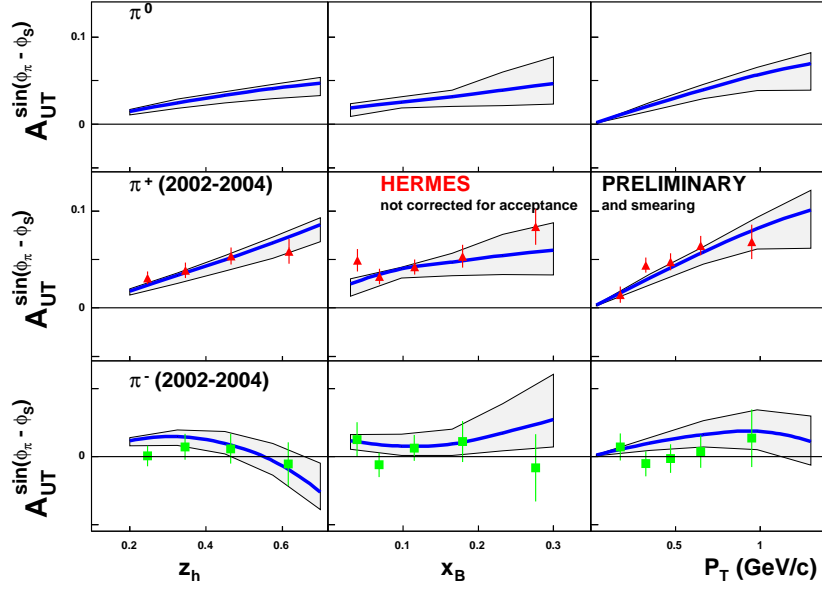


Figure 1: HERMES data on $A_{UT}^{\sin(\phi_\pi - \phi_S)}$ [7] for scattering off a transversely polarized proton target and charged pion production. The curves are the results of our fit. The shaded area spans a region corresponding to one-sigma deviation at 90% CL (see text for further detail). Predictions for π^0 (upper panel) and kaon (lower panels) asymmetries are also shown.

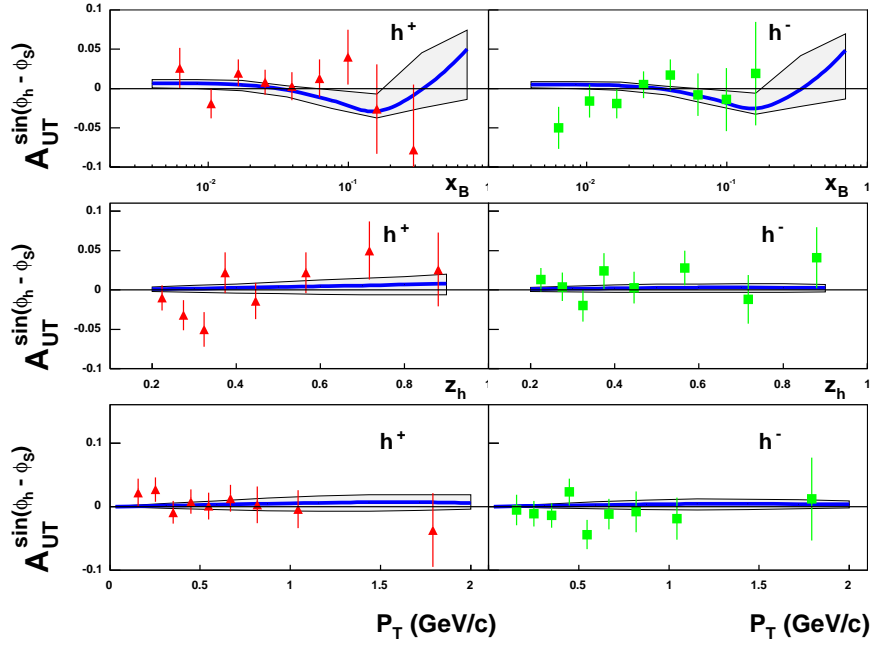


Figure 2: COMPASS data [8] on $A_{UT}^{\sin(\phi_h - \phi_S)}$ for scattering off a transversely polarized deuteron target and the production of positively (h^+) and negatively (h^-) charged hadrons. The curves are the results of our fit. The shaded area spans a region corresponding to one-sigma deviation at 90% CL (see text for further detail).

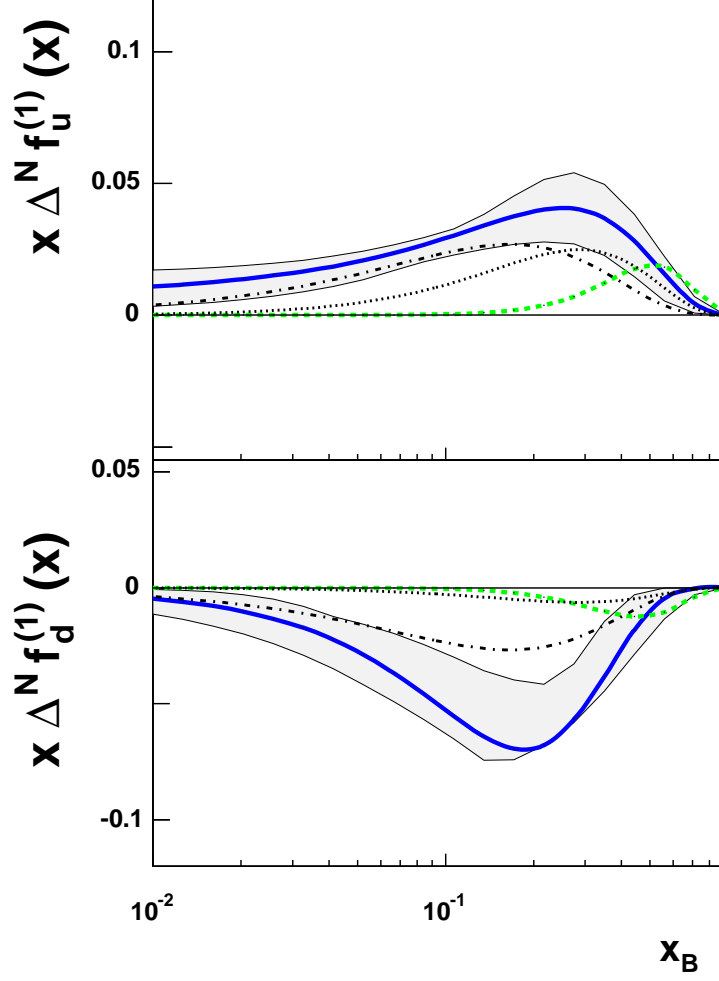


Figure 3: The x -dependence of the first \mathbf{k}_\perp moment, according to Eq. (22), of our extracted Siverts functions. The solid line is obtained by using the central values of the parameters in Table I and the shaded area corresponds to varying the parameters within the shaded areas in Figs. 1 and 2. The dot-dashed, dashed and dotted lines show the first \mathbf{k}_\perp moments of the Siverts functions obtained respectively in Refs. [13], [14] and [15].

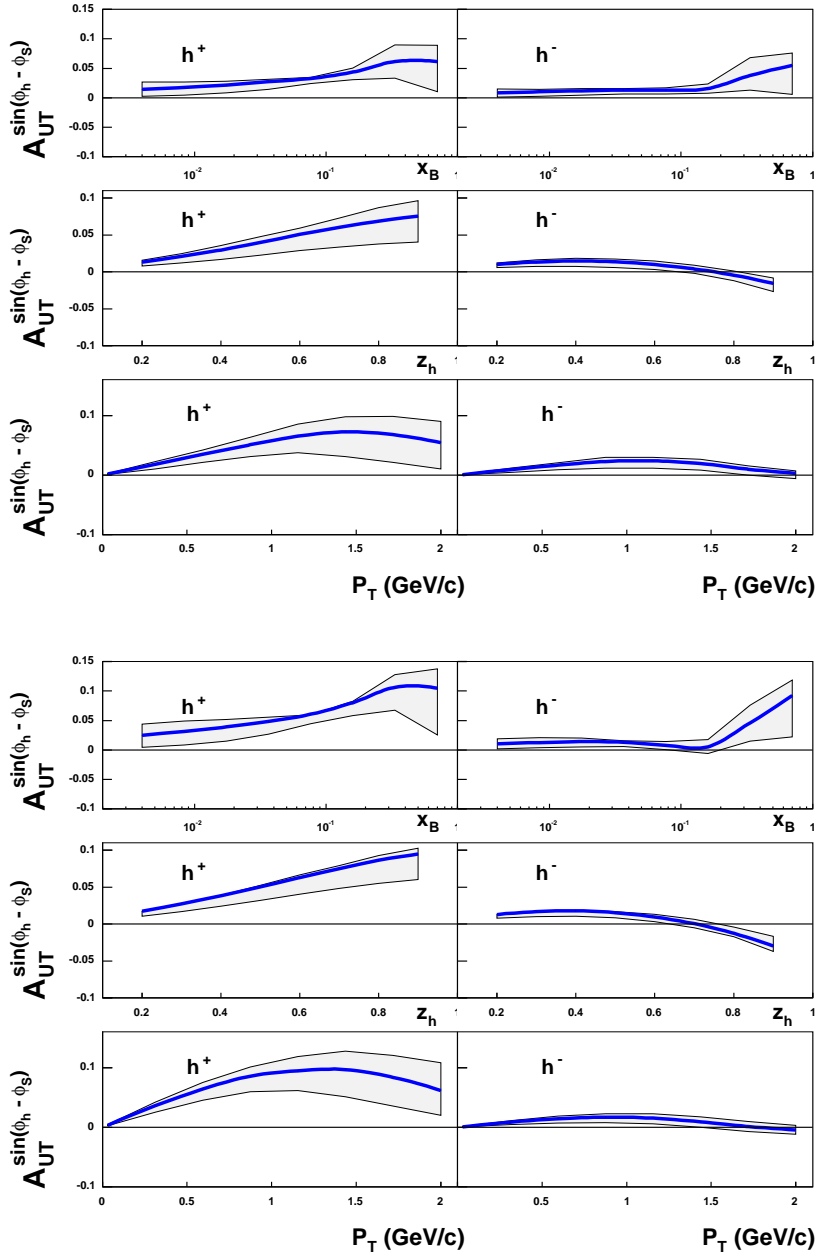


Figure 4: Predictions for $A_{UT}^{\sin(\phi_h - \phi_S)}$ at COMPASS for scattering off a transversely polarized proton target and the production of positively (h^+) and negatively (h^-) charged hadrons. The plots in the upper panel have been obtained by performing the integrations over the unobserved variables according to the standard COMPASS kinematical cuts [1]; results with suggested new cuts, Eq. (27), are presented in the lower panel.

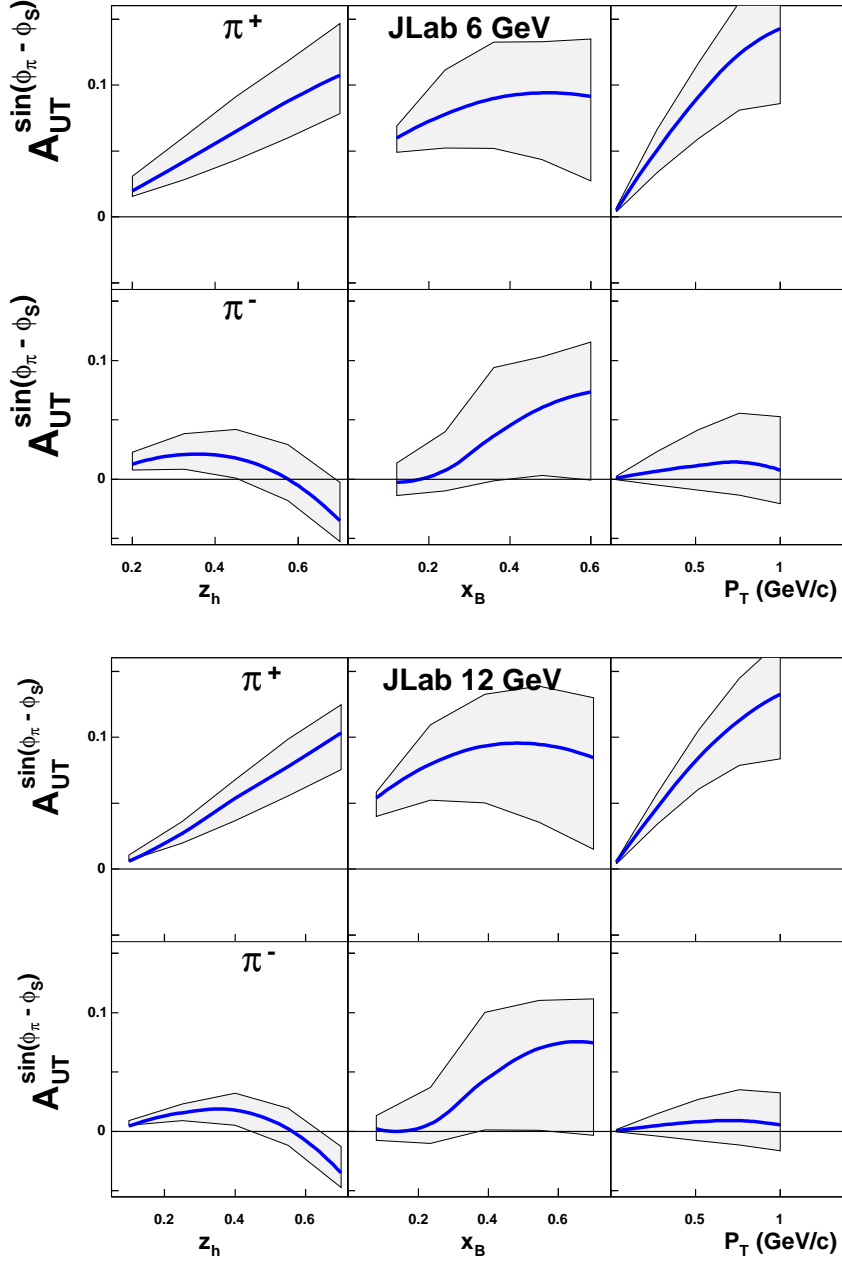


Figure 5: Predictions for $A_{UT}^{\sin(\phi_\pi - \phi_S)}$ at JLab for the production of π^+ and π^- from scattering off a transversely polarized proton target. Integrations over the unobserved variables have been performed according to the kinematical ranges of Eqs. (28) and (29).

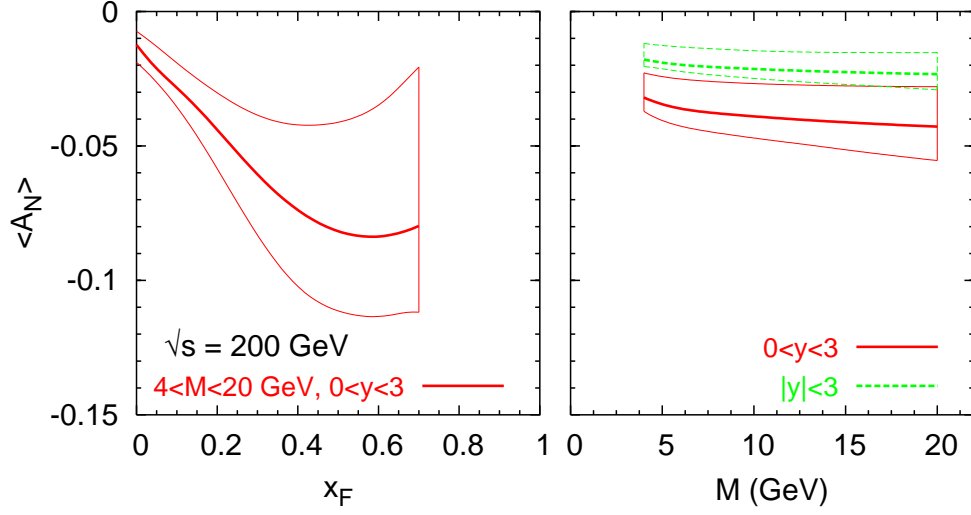


Figure 6: Predictions for single spin asymmetries in Drell-Yan processes at RHIC, $p^\uparrow p \rightarrow \ell^+ \ell^- X$, according to Eq. (32) of the text. The lepton pair transverse momentum has been integrated in the range $0 \leq q_T \leq 1$ GeV/ c ; A_N is plotted as a function of x_F (left) and M (right), with integration over the other variable as indicated in the legend (see text for further details). Values of $\langle A_N \rangle$ for negative x_F are negligible, at RHIC kinematics.

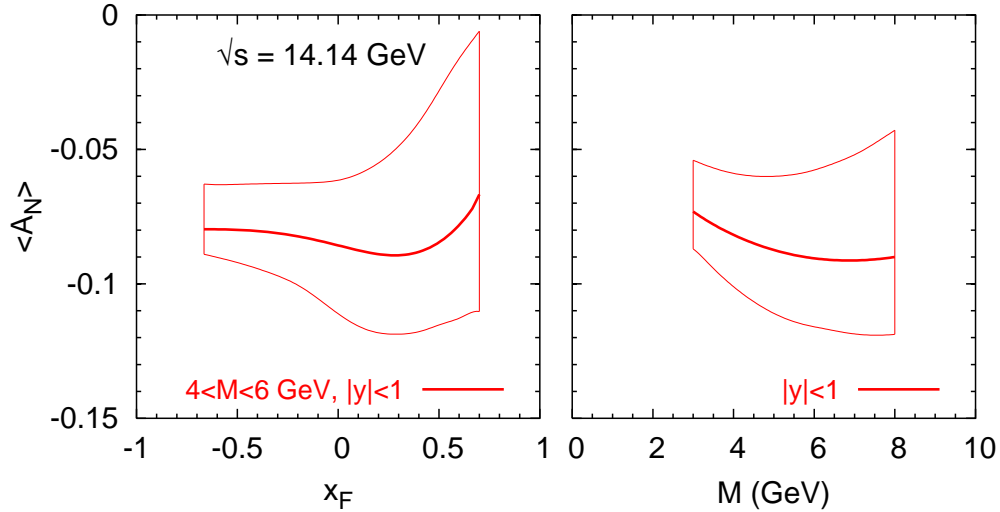


Figure 7: Predictions for single spin asymmetries in Drell-Yan processes at GSI, $p^\uparrow \bar{p} \rightarrow \ell^+ \ell^- X$, according to Eq. (32) of the text. The lepton pair transverse momentum has been integrated in the range $0 \leq q_T \leq 1$ GeV/ c ; A_N is plotted as a function of x_F (left) and M (right), with integration over the other variable as indicated in the legend (see text for further details). The results for the $\bar{p}^\uparrow p \rightarrow \ell^+ \ell^- X$ process are the same.